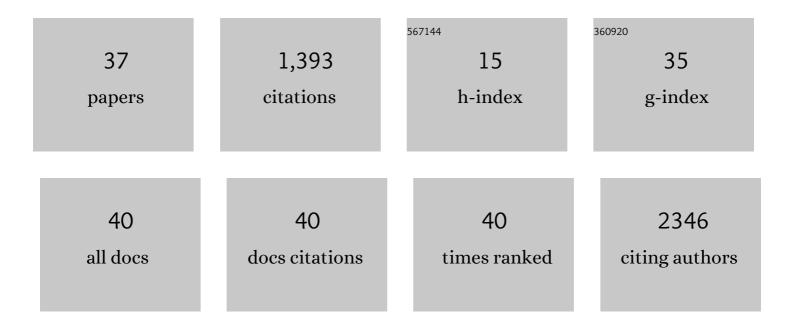
Jeetender Chugh

List of Publications by Year in descending order

Source: https://exaly.com/author-pdf/7179531/publications.pdf Version: 2024-02-01



#	Article	IF	CITATIONS
1	Inherent conformational plasticity in dsRBDs enables interaction with topologically distinct RNAs. Biophysical Journal, 2022, , .	0.2	2
2	Myricetin protects pancreatic β-cells from human islet amyloid polypeptide (hIAPP) induced cytotoxicity and restores islet function. Biological Chemistry, 2021, 402, 179-194.	1.2	22
3	Construction of Entropically Favored Supramolecular Metal–Ligand Trimeric Assemblies Supported by Flexible Pyridylaminophosphorus(V) Scaffolds. Inorganic Chemistry, 2021, 60, 10468-10477.	1.9	5
4	A Pyridyl-Linked Benzimidazolyl Tautomer Facilitates Prodigious H ⁺ /Cl [–] Symport through a Cooperative Protonation and Chloride Ion Recognition. Organic Letters, 2021, 23, 6131-6136.	2.4	13
5	Cold storage reveals distinct metabolic perturbations in processing and non-processing cultivars of potato (Solanum tuberosum L.). Scientific Reports, 2020, 10, 6268.	1.6	11
6	Solidâ€Phase Synthesis of Clickable Psicofuranose Glycocarbamates and Application of Their Selfâ€Assembled Nanovesicles for Curcumin Encapsulation. ChemistrySelect, 2020, 5, 2672-2677.	0.7	1
7	NMR analysis of nucleotide π-stacking in prebiotically relevant crowded environment. Communications Chemistry, 2020, 3, .	2.0	3
8	Palladiumâ€Catalyzed Insertion of Ethylene and 1,1â€Disubstituted Difunctional Olefins: An Experimental and Computational Study. ChemPlusChem, 2020, 85, 1200-1209.	1.3	3
9	Metabolic signatures suggest o-phosphocholine to UDP-N-acetylglucosamine ratio as a potential biomarker for high-glucose and/or palmitate exposure in pancreatic β-cells. Metabolomics, 2019, 15, 55.	1.4	16
10	1H, 13C and 15N resonance assignment of domain 1 of trans-activation response element (TAR) RNA binding protein isoform 1 (TRBP2) and its comparison with that of isoform 2 (TRBP1). Biomolecular NMR Assignments, 2018, 12, 189-194.	0.4	3
11	lmido-P(v) trianion supported enantiopure neutral tetrahedral Pd(ii) cages. Chemical Communications, 2018, 54, 1873-1876.	2.2	16
12	Origin of the Substitution Mechanism for the Binding of Organic Ligands on the Surface of CsPbBr ₃ Perovskite Nanocubes. Journal of Physical Chemistry Letters, 2017, 8, 4988-4994.	2.1	292
13	miRNAs: Nanomachines That Micromanage the Pathophysiology of Diabetes Mellitus. Advances in Clinical Chemistry, 2017, 82, 199-264.	1.8	12
14	Synthesis of barbituric acid containing nucleotides and their implications for the origin of primitive informational polymers. Physical Chemistry Chemical Physics, 2016, 18, 20144-20152.	1.3	23
15	A Neutral Cluster Cage with a Tetrahedral [Pd ₁₂ ^{II} L ₆] Framework: Crystal Structures and Host–Guest Studies. Inorganic Chemistry, 2015, 54, 3196-3202.	1.9	15
16	Engineering a Therapeutic Lectin by Uncoupling Mitogenicity from Antiviral Activity. Cell, 2015, 163, 746-758.	13.5	89
17	miRNAs: early prognostic biomarkers for Type 2 diabetes mellitus?. Biomarkers in Medicine, 2015, 9, 1025-1040.	0.6	40
18	Flipping of the Ribosomal A-Site Adenines Provides a Basis for tRNA Selection. Journal of Molecular Biology, 2014, 426, 3201-3213.	2.0	31

JEETENDER CHUGH

#	Article	IF	CITATIONS
19	Determining Transient Nucleic Acid Structures by NMR. , 2014, , 181-198.		Ο
20	Visualizing transient low-populated structures of RNA. Nature, 2012, 491, 724-728.	13.7	184
21	Functional complexity and regulation through RNA dynamics. Nature, 2012, 482, 322-330.	13.7	286
22	Characterizing RNA dynamics at atomic resolution using solution-state NMR spectroscopy. Nature Methods, 2011, 8, 919-931.	9.0	131
23	Using Fluorine Nuclear Magnetic Resonance To Probe the Interaction of Membrane-Active Peptides with the Lipid Bilayer. Biochemistry, 2010, 49, 5760-5765.	1.2	55
24	Generation of serine/threonine check points in HN(C)N spectra. Journal of Chemical Sciences, 2009, 121, 955-964.	0.7	10
25	1H, 15N, 13C resonance assignment of 9.7ÂM urea-denatured state of the GTPase effector domain (GED) of dynamin. Biomolecular NMR Assignments, 2009, 3, 13-16.	0.4	3
26	Conserved structural and dynamics features in the denatured states of drosophila SUMO, human SUMO and ubiquitin proteins: Implications to sequenceâ€folding paradigm. Proteins: Structure, Function and Bioinformatics, 2009, 76, 387-402.	1.5	8
27	NMRâ€derived solution structure of SUMO from <i>Drosophila melanogaster</i> (dSmt3). Proteins: Structure, Function and Bioinformatics, 2009, 75, 1046-1050.	1.5	4
28	Comparison of NMR structural and dynamics features of the urea and guanidine-denatured states of GED. Archives of Biochemistry and Biophysics, 2009, 481, 169-176.	1.4	6
29	Tuning the HNN experiment: generation of serine–threonine check points. Journal of Biomolecular NMR, 2008, 40, 145-152.	1.6	17
30	1H, 15N, 13C resonance assignment of folded and 8ÂM urea-denatured state of SUMO from Drosophila melanogaster. Biomolecular NMR Assignments, 2008, 2, 13-15.	0.4	9
31	Spectroscopic labeling of A, S/T in the 1H–15N HSQC spectrum of uniformly (15N–13C) labeled proteins. Journal of Magnetic Resonance, 2008, 194, 289-294.	1.2	6
32	Effect of a single point mutation on the stability, residual structure and dynamics in the denatured state of GED: Relevance to self-assembly. Biophysical Chemistry, 2008, 137, 13-18.	1.5	2
33	Equilibrium Refolding Transitions Driven by Trifluoroethanol and by Guanidine Hydrochloride Dilution Are Similar in GTPase Effector Domain: Implications to Sequenceâ^'Self-Association Paradigm. Biochemistry, 2008, 47, 12945-12953.	1.2	2
34	NMR insights into a megadaltonâ€size protein selfâ€assembly. Protein Science, 2008, 17, 1319-1325.	3.1	15
35	Pockets of Short-Range Transient Order and Restricted Topological Heterogeneity in the Guanidine-Denatured State Ensemble of GED of Dynamin. Biochemistry, 2007, 46, 11819-11832.	1.2	20
36	Structural characterization of the large soluble oligomers of the GTPase effector domain of dynamin. FEBS Journal, 2006, 273, 388-397.	2.2	22

#	Article	IF	CITATIONS
37	NMR of unfolded proteins. Journal of Chemical Sciences, 2005, 117, 3-21.	0.7	15